Hindawi
Advances in Materials Science and Engineering
Volume 2022, Article ID 4913887, 13 pages
https://doi.org/10.1155/2022/4913887

Research Article

Effect of Pile-Soil Relative Stiffness on Deformation Characteristics of the Laterally Loaded Pile

Bingxiang Yuan, Minjie Chen, Weijie Chen, Qingzi Luo, and Hongzhong Li

School of Civil and Transportation Engineering, Guangdong University of Technology, Guangzhou, Guangdong 510006, China

Correspondence should be addressed to Qingzi Luo; lqz1986@gdut.edu.cn

Received 2 February 2022; Accepted 1 April 2022; Published 12 May 2022

Academic Editor: Aniello Riccio

Laterally loaded piles are widely used in structural foundations under horizontal loads such as wave load, wind load, seismic load, and traffic load. Based on the complexity of pile-soil interaction, a test simulation of single pile through the indoor 1 g model test was conducted, in order to study the influence of different loading heights and relative stiffness of pile and soil on the bending moment, soil resistance, and horizontal displacement of pile. It is found that the shear modulus of soil from large to small is arranged as dry fine sand, dry coarse sand, saturated fine sand, and saturated coarse sand. The shear modulus of dry fine sand, dry coarse sand, and saturated fine sand are close under the same loading height and horizontal displacement of pile top, while the shear modulus of saturated coarse sand decreases sharply. Under the condition of water saturation, the particle size has a significant effect on the shear modulus of soil. The relative stiffness of pile soil is found to be the main influencing condition of pile horizontal displacement. Compared with the displacement and bending moment of the pile, the loading height has more influence on the soil resistance, and the main influence area is the soil resistance of the pile toe.

1. Introduction

In recent decades, laterally loaded piles have been widely used in high-rise buildings, long-span bridges, and large offshore wind power structures. The influence of lateral force, different from other pile foundations that only consider the vertical force in the design, should be considered in the design of horizontally loaded piles [1–3]. The pile body will produce force deformation under horizontal load, resulting in lateral displacement of soil. With the increase of lateral displacement of soil, the constraint of pile also increases. The coupling effect between pile and soil forms a complex pile-soil interaction [4–6].

There are many factors affecting pile-soil interaction, including pile material characteristics, geometry, and soil characteristics, which reflect the complexity of the pile-soil interaction [7–9]. Complicated behavior of pile-soil interaction through theoretical analysis, numerical simulation, and indoor model test have been studied by many domestic and foreign scholars. Based on the fact that API rules are not applicable to large-diameter single pile, Liu and Zhu [10, 11] introduced the secant stiffness attenuation model of sandy soil. Combined with the laboratory test and finite element model, the critical depth of pile foundation under horizontal cyclic load of super large diameter pile was deduced theoretically [12–14]. A series of 1 g small-scale models of different sand densities, of varying pile lengths and pile diameters, and of several pile section geometry and pile stiffness were carried out by Uncuoglu to study the influence of different factors on the lateral bearing capacity of pile. His study concluded that soil density has the most obvious effect on lateral bearing capacity of pile [15]. Under the same relative density, the lateral displacement resistance and bending moment of piles in unsaturated soil are lower than those in the saturated state, which is caused by the suction effect in unsaturated soil [16]. In saturated clay, increasing the buried depth of pile foundation is conducive to the long-term bearing stability of single pile, while excessively increasing the diameter of pile reduces the bearing capacity of horizontal loaded pile [17]. Shi et al. conducted a centrifugal test and analyzed the dynamic response of pile-soil interaction of 2×2 piles under lateral cyclic loading in clay [18].

The pile group was found to be unable to return to its original position after applying each loading and unloading cycle, for the reason that the cyclic load induces plastic deformation in the soil around the pile and there is bending strain in the pile group [19–21]. Compared with the study of horizontal loading of pile groups, the discussion of eccentric loading is more general. Kong et al. [16] expounded the motion law of two piles under horizontal eccentric load and carried out model test and numerical simulation to obtain the calculation method of generalized p-multiplier. The algorithm was finally verified in an engineering example [22]. In addition, with the development of particle image velocimetry technology, the study of the visual indoor 1g scale model test can better analyze the response of pile-soil interaction [23–25].

Based on the existing research results, the conditions of different loading points in dry sand and saturated sand (loading at the height of 2.1D and 6D respectively, where D is the pile diameter) through indoor test were performed in this study, so as to obtain the results of pile bending moment, horizontal displacement, and stress distribution of pile soil through displacement loading. The effects of the changes of pile-soil relative stiffness on the pile-soil mechanical response of laterally loaded piles in sand were then analyzed.

2. Method and Materials

2.1. Test Device and Model Pile. Based on the existing research of the indoor scale test model, the influence of soil boundary on the pile-soil interaction model can be ignored when the design distance between laterally loaded single pile and boundary is greater than 6 times of pile diameter [26–28]. Thus, the model size of this test was 360 mm long, 240 mm wide, and 490 mm high. Moreover, a filter inlet was installed at the bottom of the test tank. In order to better observe the surface smoothness and saturation of soil, the material of the test tank was selected as an acrylic glass plate. The test tank was placed on the fabricated steel frame for better fixing the loading point position of the pile. Moreover, the test tank was equipped with two height bases for loading at different heights.

A single pile, with a diameter of 2.5 m, a wall thickness of 0.045 m, a buried depth of 50 m, a pile length of 65 m, and a corresponding bending stiffness of 56.66 GN·m^2 was used as the prototype pile in this test. Considering the similarity ratio and the boundary effect of the test tank, the size similarity ratio (λ_1) of 1 : 130 was selected for indoor scale test. Based on the previous analysis of the 1g model test of horizontal loaded piles [29–31], the parameters and similarities between the model and the prototype pile are shown in Table 1. The size of the model pile was set to be 19 mm in diameter, 1.5 mm in wall thickness, 38.5 cm in depth, and 50 cm in length according to the similarity ratio.

2.2. Test Material. The soil material used in this indoor model test was Fujian sand with a particle size less than 2 mm. In order to explore the influence of particle size on laterally loaded piles, Fujian sand was divided into two groups with particle size less than 1 mm (hereinafter collectively referred to as fine sand) and 1-2 mm (hereinafter collectively referred to as coarse sand). Based on the geotechnical test method standards, the specific gravity, relative density, and particle gradation tests of coarse sand and fine sand were carried out, respectively. The basic physical parameters of the soil obtained from the test are shown in Table 2 and the particle gradation is shown in Figure 1.

Table 1: Similarity ratio between the model pile and prototype pile.

Physical quantity	Similarity ratio	Prototype pile	Model pile
Pile length	λ_1	65m	50 cm
Embedded depth	λ_1	50m	38.5 cm
Calculation diameter	λ_1	2.5 m	1.9 cm
Bending stiffness	${\lambda_1}^4$	56.66 GN·m^2	198 N·m^2
Horizontal load	${\lambda_1}^2$		

According to the particle grading curve (Figure 1), d_{10}, d_{30}, and d_{60} of Fujian standard sand used in the test are 0.17 mm, 0.4 mm, and 0.9 mm, respectively. It can be determined that the coefficient of uniformity C_u of Fujian standard sand used in this test is 5.29 and the coefficient of curvature C_C is 1.05. It can be seen that the sand is well graded.

2.3. Data Acquisition and Loading Equipment. Two loading points were designed at 6D and 2.1D away from the ground surface, and nine pairs of strain gauges were set on the pile body, one of which was 2.4 cm above the ground surface, and the other eight pairs of strain gauges were below the ground (Figure 2).

The stepping motor was used in this test and applied horizontal load to the pile, with the loading rate of 0.083 cm/s and the displacement amplitude of 0.012 m. The bending strain generated by horizontal loading was connected to the computer by a Donghua DH-3818N-2 static strain tester and collected by a DHDAS dynamic signal acquisition and analysis system. A camera was set up at the top of the test chamber (Figure 3).

2.4. Test Procedure. Two test parameters were changed in this indoor 1g test, namely, changing the loading height (2.1D, 6D) and changing the soil stiffness conditions (dry fine sand, dry coarse sand, water saturated fine sand, and water saturated coarse sand). A total of 8 groups of tests were carried out. The pile-soil mechanical response of laterally loaded piles was studied by changing the test parameters.

During the test, in order to ensure that the relative compactness requirements required by the test are met, the sand is filled several times. The test sand was uniformly loaded in the middle along the inner wall of the test tank through the funnel. When the first layer of sand has been completely filled through the funnel, the height of the sand, generally was not flush with the scale line. In order to ensure that the height of the sand was flush with the scale line and

Table 2: Physical parameters of Fujian sand.

Particle size range (mm)	Proportion ds -	Minimum dry density ρdmin (g/cm^3)	Maximum dry density ρdmax (g/cm^3)	Minimum void ratio emin -	Maximum void ratio emax -
0–1	2.64	1.43	1.88	0.40	0.85
1–2	2.64	1.43	1.75	0.50	0.85

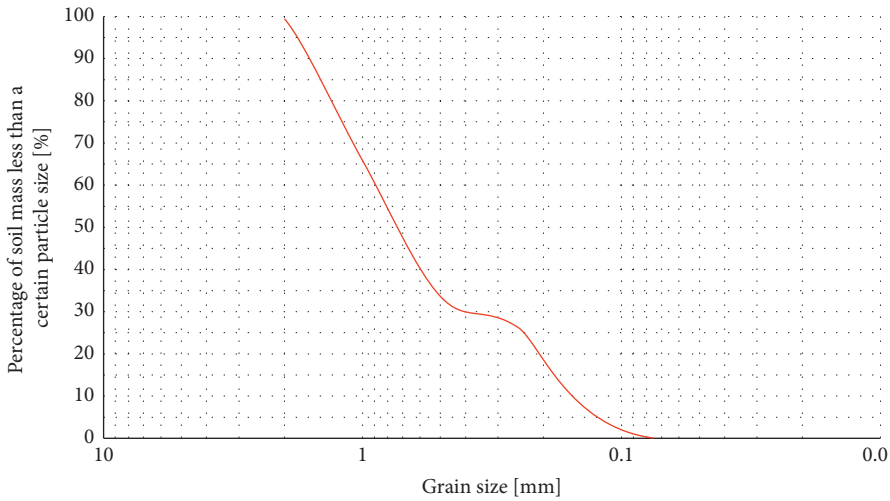

Figure 1: Grading curve of Fujian standard sand.

that the compactness of the test met the requirements, the sand in the test tank could be scraped back and forth several times with cardboard, and then the self-made small round roller could be used to compact the height of the sand to the specified height at a slow speed. After the first layer of sand was filled to the specified scale line, the model pile was placed in the center of the test tank by diagonal method, and the heavy hammer was used to ensure that the pile is in a vertical state. The sand was filled in layers according to the above filling method to the scale mark corresponding to the pile embedded depth of 38.5 cm. The soil should be placed for 6h before the test after the sand filling is completed.

3. Results and Discussion

3.1. Analysis of the Pile Top Displacement and Load. Lateral loading tests of dry fine sand, dry coarse sand, saturated fine sand, and saturated coarse sand at 6D and 2.1D heights were carried out, respectively. The horizontal displacement at the top of the model pile under various loads was obtained by a laser displacement meter at the soil surface. The test results are shown in Figure 4. It can be seen from Figure 4 that with the increase of lateral load, the horizontal displacement of the pile in the saturated coarse sand group under different height loading conditions is significantly greater than that of the other six groups of tests. In addition to the saturated coarse sand group, the other six groups of tests showed a similar trend of horizontal displacement-load curve of pile top at the same loading height. Under the same load, the horizontal displacement of pile top at 6D loading point is obviously larger than that at 2.1D loading point. According to the internal force equilibrium condition between cantilever beam and fixed end, tilting moment can be simplified as follows:

$$M = H \cdot e, \tag{1}$$

where e is the loading height and H is the horizontal load acting on the pile. It can be seen from (1) that the greater the loading height, the greater the corresponding overturning moment. The overturning moment will be coupled with the lateral load, and the overturning moment generated by the lateral load will reduce the horizontal bearing capacity of the pile. Thus, under the same load conditions, the higher the loading point, the greater the horizontal displacement. It can be explained that the slopes of the experimental groups with other sand conditions at 2.1D loading height are smaller than those of the corresponding experimental groups at 6D loading height, except the two groups of experiments with saturated coarse sand in Figure 4. The weakening effect of soil shear strength is significantly higher than that of loading height due to the low shear strength of saturated coarse sand group [32–34]. Thus, the slopes of the two groups of saturated coarse sand are similar. The horizontal displacement of pile top in dry fine sand group is the smallest under the same lateral load, followed by the dry coarse sand group and saturated fine sand groups. It is observed that the shear strength of fine sand under saturated condition is greater than that of saturated coarse sand group. This is because the larger the particle size under saturated condition, the larger the pore water flow channel, which will greatly attenuate the shear modulus of soil.

Under the same loading height, the horizontal displacement curves of pile top at 0.05D, 0.1D, 0.15D, 0.2D, 0.25D, 0.3D and 0.4D were taken respectively to compare

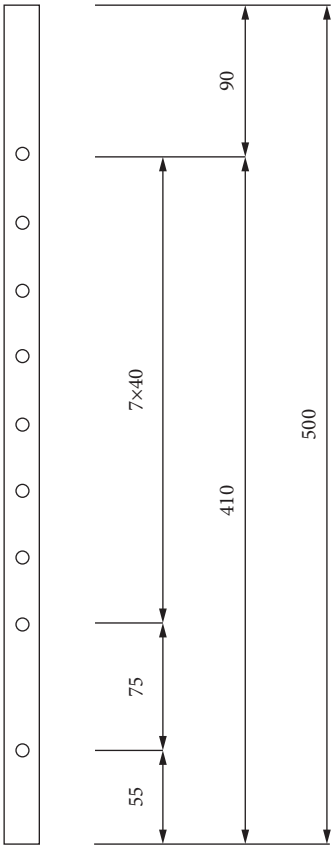

Figure 2: Schematic diagram of pile (mm).

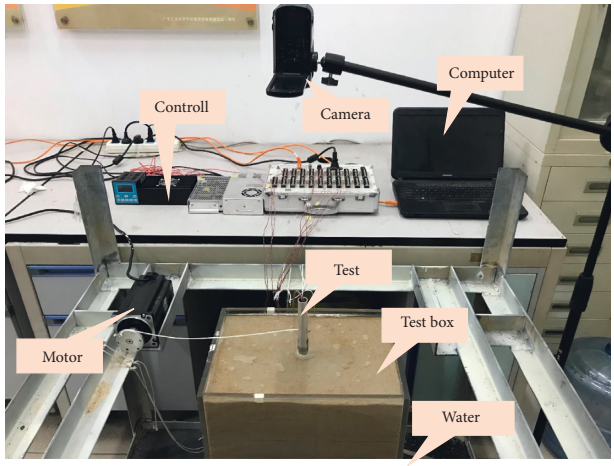

Figure 3: Test device diagram.

and analyze the influence of soil stiffness and soil layer on the change of pile horizontal displacement (Figure 5). As shown in Figures 5(a) and 5(b), under the same loading height, the pile displacement of dry fine sand group is similar to that of dry coarse sand group. It can also be seen from the Fig. that the horizontal displacement of dry fine sand group is less than that of coarse sand group in a certain range of surface.

It can be noted that the horizontal displacement between saturated fine sand and saturated coarse sand is quite different, especially when the loading height is 6D. Under

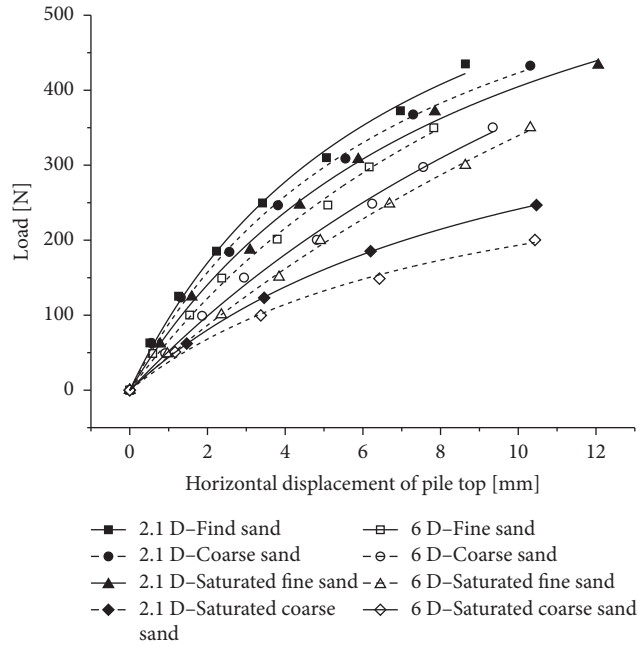

Figure 4: Horizontal displacement-load curve of pile top. Analysis of pile displacement and load.

different loading heights, the horizontal displacement of pile in saturated fine sand group is less than that in saturated coarse sand group. Comparing the horizontal displacement of the pile end of the 6D loading coarse sand group shown in Figure 5(d) with that of other test groups, there is a phenomenon that the horizontal displacement curve of the pile body with the horizontal displacement of the pile top of 0.4D moves to the right. It is also seen from Figure 5(d) that the slope of the horizontal displacement curve of the pile body is similar below the pile buried depth of 0.25 m, but there is a great difference above the buried depth of 0.25 m. This is due to the rotation and translation of the pile in saturated coarse sand under large load, and the relative rotation point of the pile end is bent forward, and the relative bending moment is large. The horizontal displacement of the pile body is obtained by fitting the bending moment with the formula of 6 times [35, 36]. Thus, compared with the previous groups of tests, the horizontal displacement curve of the pile body bends inward when the horizontal displacement of the pile top is 0.4D.

It is observed from Figure 6 that the loading height has little effect on the horizontal displacement of the pile. According to the sequence of dry fine sand, dry coarse sand, saturated fine sand, and saturated coarse sand, it can be found that the maximum horizontal displacement of the pile at 2.1D loading height is first less than, approximately equal to, slightly greater than or greater than the group of 6D loading height. This phenomenon is similar to the shear strength of soil, showing the deformation characteristics of flexible piles. The increase in deflection of pile section above the ground surface is attributed to the increased shear strength of soil and the increased loading height. Due to the existence of soil, the deflection of pile section below the ground surface is smaller than that above the surface

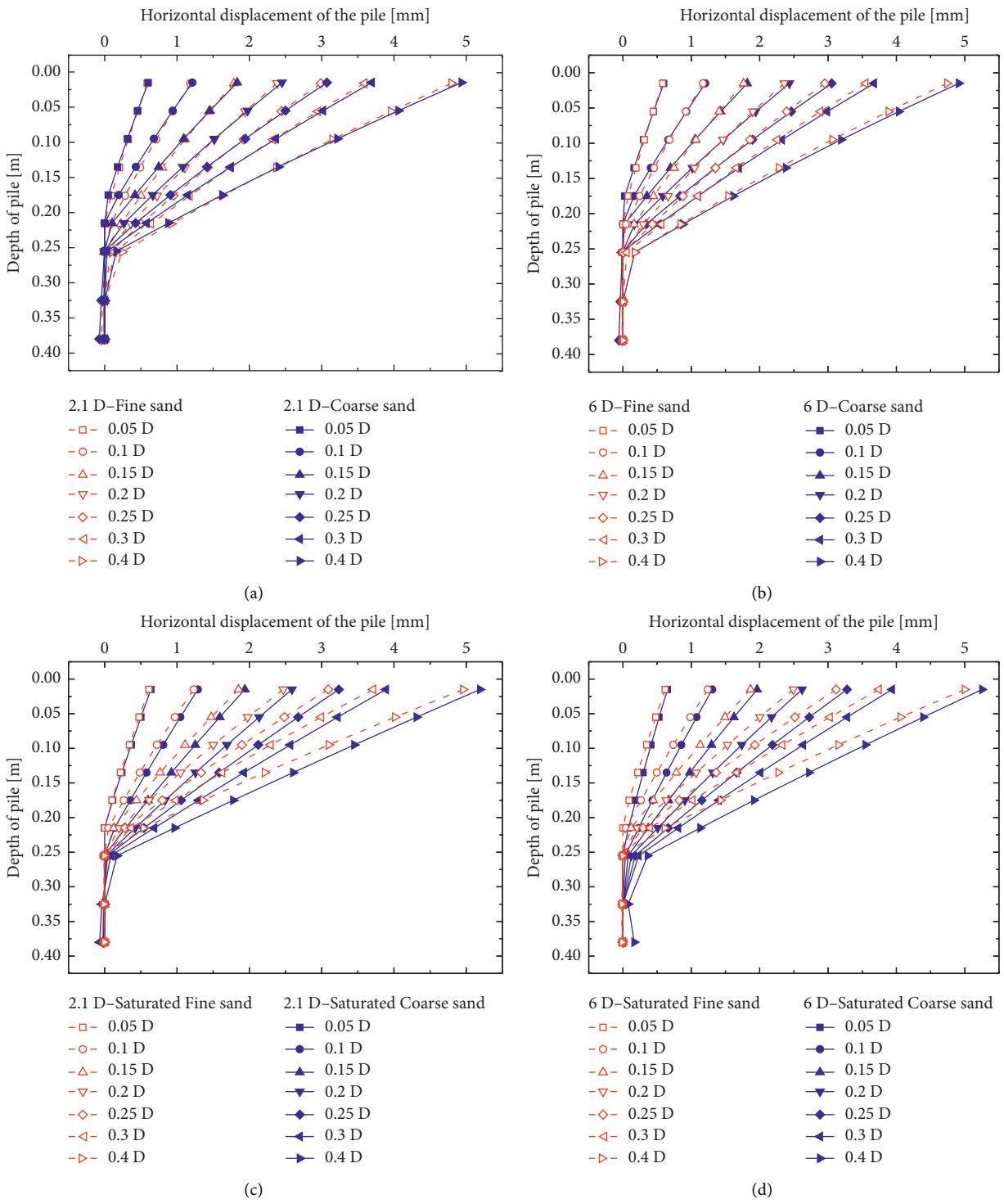

Figure 5: Comparison of pile displacement in fine sand and coarse sand. (a) 2.1D dry sand, (b) 2.1D dry sand, (c) 2.1D saturated sand, and (d) 6D saturated sand.

[37–39]. The above displacement curves of pile body, no matter the difference of loading height or the difference of pile-soil relative stiffness, show the deformation characteristics of partial flexible piles and partial rigid piles, that is, the model piles in this paper are semirigid piles in the test. The displacement of the pile is obtained by the second derivative fitting of the bending moment obtained by the test mentioned above, resulting in the pile displacement curve of the pile end approximate to the fixed support.

3.2. Analysis of the Pile Bending Moment. The horizontal displacement of pile top as 0.05D, 0.1D, 0.15D, 0.2D, 0.25D, 0.3D, and 0.4D were took, respectively, for analysis and

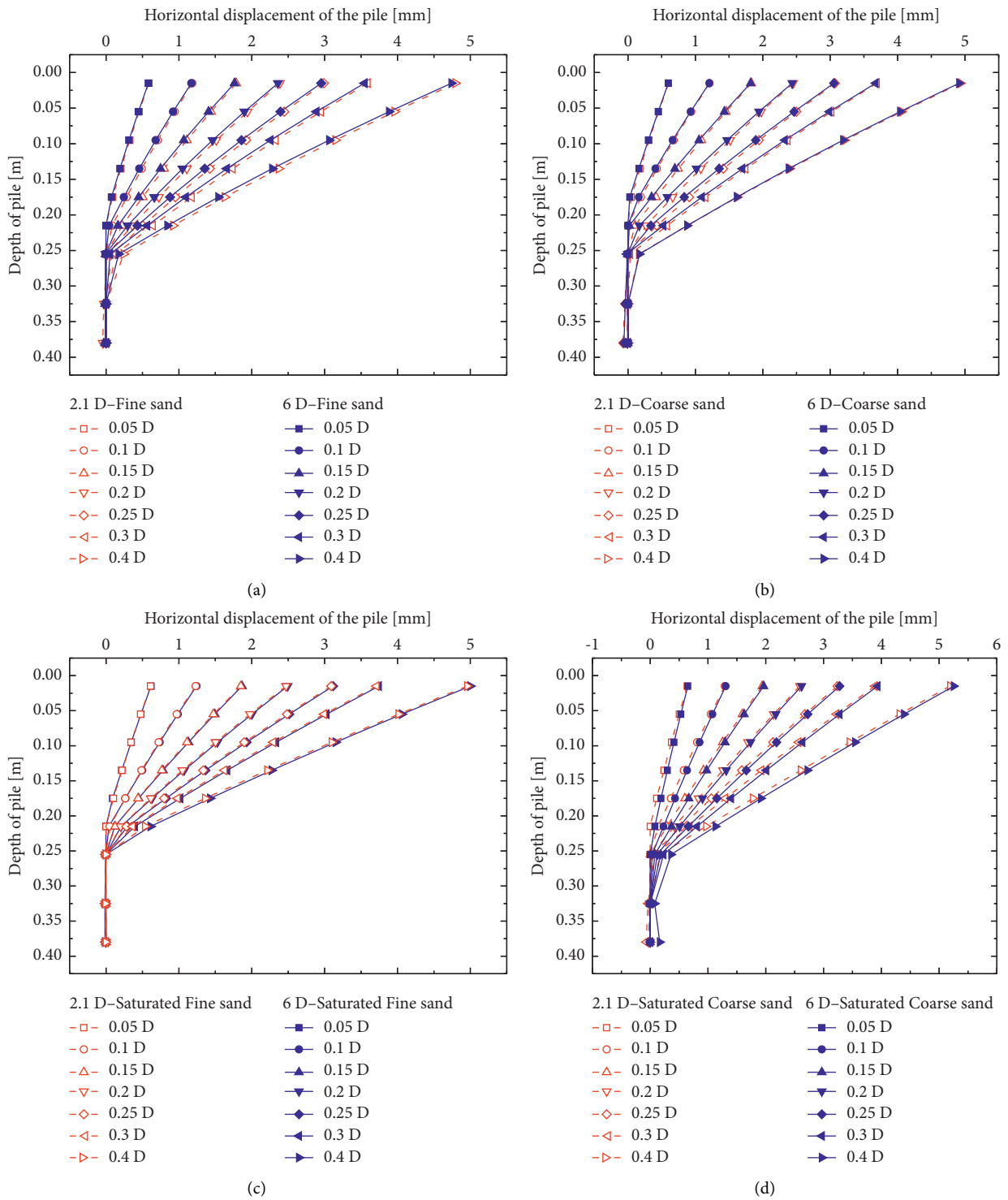

Figure 6: Comparison of pile displacement under different loading heights. (a) Fine sand, (b) coarse sand, (c) saturated fine sand, and (d) saturated coarse sand.

comparison of bending moment (Figure 7). The bending moment of pile was analyzed by loading height and sand conditions.

It is observed that the maximum bending moment of coarse sand is less than that of fine sand under dry and saturated conditions and different loading heights. Comparing Figures 7(a) and 7(b), when the loading height of the bending moment curve is 6D, due to the large bending moment, the bending moment difference under the same displacement is significantly greater than the loading height of 2.1 d, which is also in line with the conclusion of overturning bending moment mentioned above. Under the same horizontal

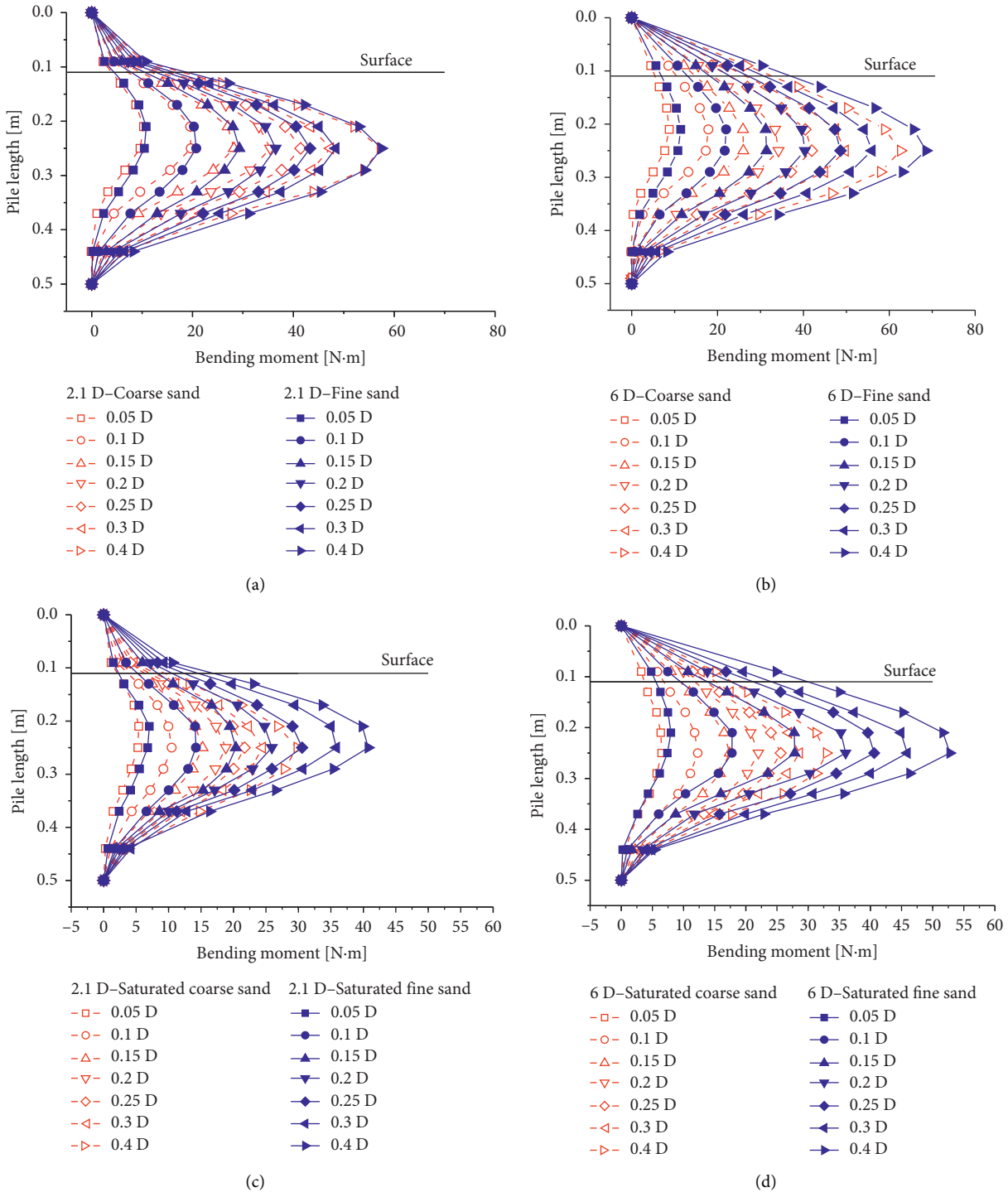

Figure 7: Comparison of bending moment in fine and coarse sand, (a) 2.1D dry sand, (b) 6D dry sand, (c) 2.1D saturated sand, and (d) 6D saturated sand.

displacement, the increase of loading height leads to the increased corresponding overturning moment. The same results are shown in Figures 7(c) and 7(d). The comparison between Figures 7(a) and 7(c), Figures 7(b) and 7(d) shows that the attenuation degree of shear strength of saturated coarse sand is significantly greater than that of fine sand, especially when the lateral load increases, the horizontal displacement difference increases significantly. The main reason is that coarse sand has larger pores and larger water volume per unit volume than fine sand, so its shear strength is low. The permeability of coarse sand is greater than that of fine sand [40–42]. Thus, when the pile moves laterally, the free water in coarse sand flows more easily. When the load is small, the maximum bending moment point of all test groups is between 0.2 m and 0.25 m. With the

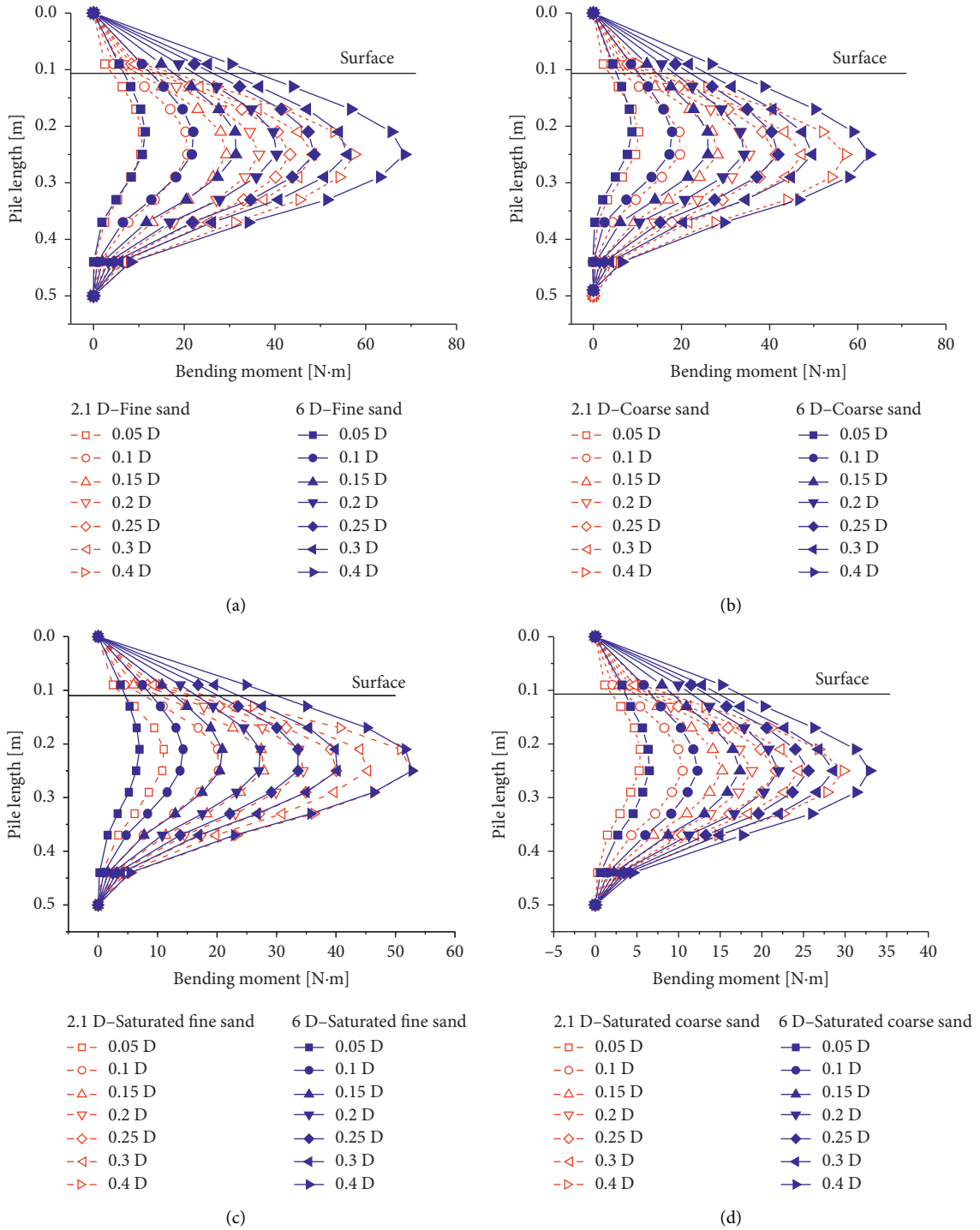

FIGURE 8: Comparison of pile bending moment with different loading height. (a) Fine sand, (b) coarse sand, (c) saturated fine sand, and (d) saturated coarse sand.

increase of horizontal displacement, namely, the increase of lateral load, the maximum bending moment point is between 0.25 m and 0.3 m. The reason is that the soil depth affected by small initial lateral load is small. With the increase of the lateral load, the influence depth increases, which makes the maximum bending moment point move down.

The bending moment was discussed and analyzed under the same soil stiffness. The bending moment curve of 6D loading height of saturated coarse sand group in Figure 8(d) envelopes the bending moment curve of 2.1D loading height. However, in other test groups, the bending moment of 2.1D loading height test group is greater than that of 6D loading height in a certain area near the pile end. In the fine sand group test, before the horizontal displacement of pile top reaches 0.3D, the bending moment at the lower part of pile body under 6D loading height is less than 2.1D loading

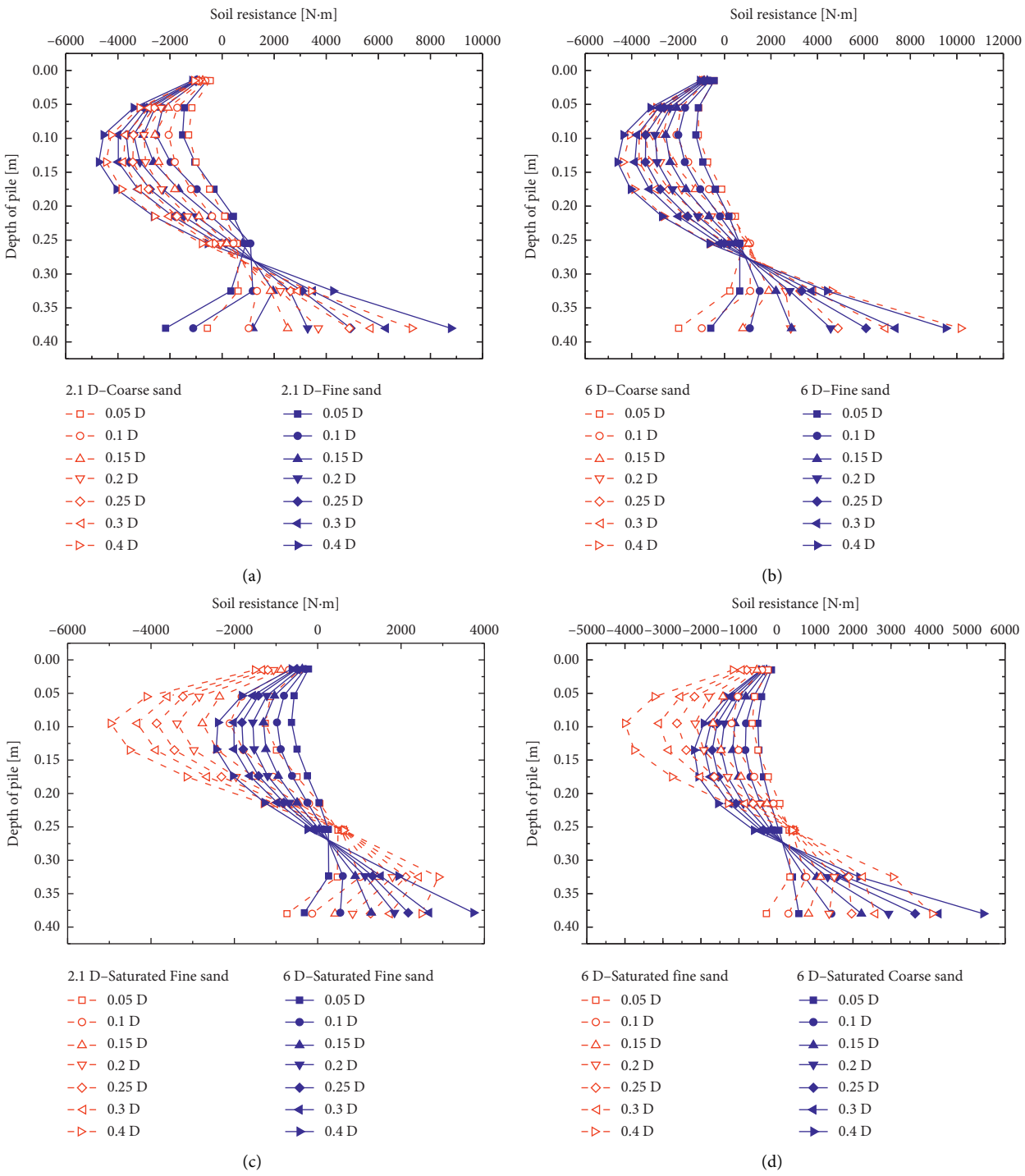

FIGURE 9: Comparison of pile soil resistance in fine and coarse sand. (a) 2.1D dry sand, (b) 6D dry sand, (c) 2.1D saturated sand, and (d) 6D saturated sand.

height. As shown in Figure 8(a), with the increase of the displacement of the pile top, the bending moment curve of the lower part of the pile under different loading heights is gradually close. Bending moment of 6D loaded fine sand group is greater than 2.1D loaded fine sand group. Figure 8(b) shows that in the coarse sand test group, when the horizontal displacement of the pile top reaches 0.3D, the bending moment of the lower part of the pile is also smaller than that of the coarse sand group with the loading height of 2.1D; nevertheless, when the horizontal displacement of the pile top reaches 0.3D, it is smaller than that of the coarse sand group with the loading height of 2.1D. It is observed from Figure 8(c) that in the saturated fine sand test group, the bending moment of the lower part of the pile under 6D loading height is still smaller than that of the fine sand group under 2.1D loading height when the horizontal displacement

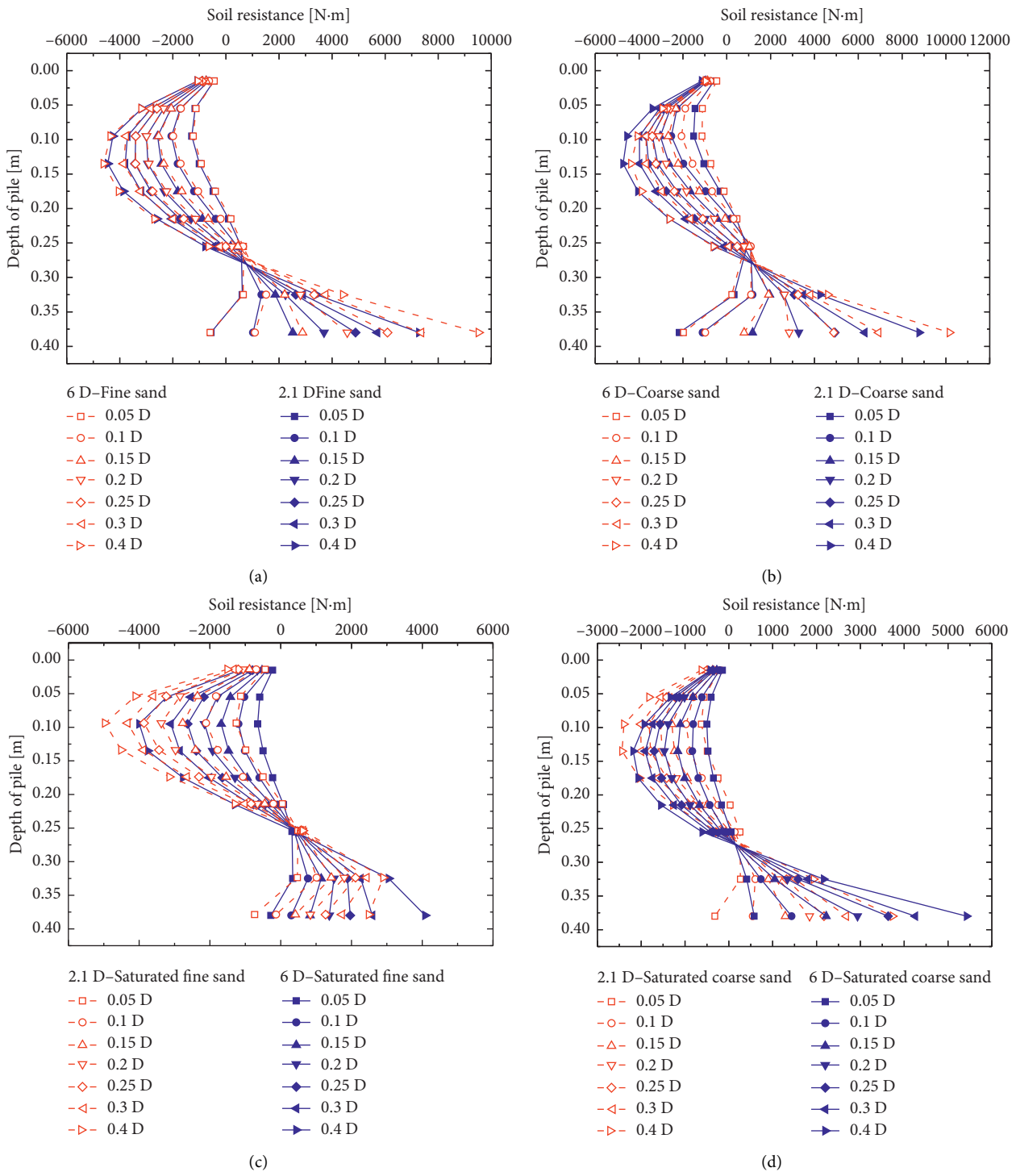

FIGURE 10: Comparison of pile soil resistance under different loading heights. (a) Fine sand, (b) coarse sand, (c) saturated fine sand, and (d) saturated coarse sand.

of the pile top is 0.4D. It can be seen that the intersection of the 2.1D loading height test group and the 6D loading height test group moves down with the increase of the horizontal displacement of the pile top. The intersection lines of dry fine sand group, dry coarse sand group and saturated coarse sand group move up in turn for the reason that the decrease of soil shear strength leads to the decrease of soil resistance provided by shallow soil under the same horizontal displacement of pile top, and the rotation point moves downward [43–45]. This leads to an increase in the depth of influence, and the soil resistance of deep soil is greater, thus the lower bending moment increases. The shear strength of saturated coarse sand is relatively low, and the influence depth under small load is greater than that of other test

groups, so Figure 8(d) displays that the bending moment curve of 6D loading height envelopes the bending moment curve of 2.1D loading height.

The analysis of the above phenomena can further illustrate that the order of shear strength from strong to weak is fine sand, coarse sand, saturated fine sand, and saturated coarse sand.

3.3. Analysis of Soil Resistance of the Pile. Similarly, under the same horizontal displacement of pile top, the influence of different loading height and different pile-soil relative stiffness on pile-soil resistance was analyzed. Figure 9 shows the comparison of soil resistance of different pile-soil relative stiffness under the same loading height.

As shown in Figures 9(a) and 9(b), the maximum soil resistance above zero point of the dry fine sand group and the dry coarse sand group is about 5000 Nm, and the maximum soil resistance at the pile end is about 10000 Nm. The result of dry fine sand test group shows that, when the horizontal displacement of the pile top reaches 0.05 d, the pile end soil resistance is greater than 0, and after the horizontal displacement of the pile top exceeds 0.1D, the pile end soil resistance is less than 0. The maximum soil resistance above zero point of the dry fine sand group is greater than that of the dry coarse sand group, but at the pile end, the maximum soil resistance of the dry coarse sand group is first less than that of the dry fine sand group and then greater than that of the dry fine sand group. The same phenomenon can also be observed in the diagram of resistance comparison between saturated fine sand and saturated coarse sand shown in Figures 9(c) and 9(d). This phenomenon is considered in two parts according to the relative magnitude of soil resistance at pile end. Shallow soil is the main bearing area. When the horizontal displacement of pile top is small, the soil under different conditions has no obvious shear failure, and the soil with larger shear strength leads to larger soil resistance [46–48]. With the increase of horizontal displacement of pile top, the influence depth increases, and the difference of shear strength between soil is reflected. Since the shear strength of dry fine sand is larger than that of dry coarse sand, the soil resistance provided by the shallow soil of dry fine sand is greater than that of dry coarse sand. The soil resistance of insufficient dry coarse sand is provided by the pile end, which also indicates that the horizontal displacement of the pile end of dry coarse sand is greater than that of dry fine sand when the horizontal displacement of the pile top is large.

The maximum soil resistance above zero point of soil resistance of saturated fine sand group in Figures 9(c) and 9(d) is between 4000 and 5000 Nm, the maximum soil resistance at pile end is between 2000 and 4000 Nm, and the corresponding maximum soil resistance of saturated coarse sand group is about 2000 Nm and 4000–6000 Nm, respectively. The maximum soil resistance above zero point of saturated coarse sand is significantly less than that of dry fine sand, dry coarse sand group and saturated fine sand group, while the maximum soil resistance of saturated fine sand group and saturated coarse sand group is significantly less than that of dry fine sand group and dry coarse sand group. Under saturated condition, there will be void at the back of the pile. Thus, the soil in the direction of active soil resistance is easier to move than the dry sand test group, and the soil resistance at the pile end is smaller.

The comparison diagram of pile-soil resistance under different loading heights under the same pile-soil relative stiffness is shown in Figure 10. In comparison of different loading heights of all test groups, the soil resistance of pile end under 6D loading height is greater than that under 2.1D loading height under the same relative stiffness of pile and soil. The position of zero rotation point of soil resistance is very close, indicating that the loading height does not affect the position of zero point of soil resistance. It is found that the soil resistance above zero and close to the surface in the 2.1D loading height test group is higher than that in the 6D loading height test group. It indicates that the soil resistance near the surface decreases with increase in the loading height, and the soil resistance at the pile end will further increase. Since the pile in this test is a semi-rigid pile, with the increase of the horizontal displacement of the pile top, the horizontal displacement of the pile end will also increase accordingly [49–51]. The increase of the loading height leads to the increase of the bending moment, so that the soil resistance generated by the soil increases to resist the pile displacement.

4. Conclusions

The effects of relative stiffness of pile and soil and different loading height on horizontal displacement, bending moment, and soil resistance of pile are studied, respectively, through the indoor 1 g test. Based on the experimental results, the following conclusions are arrived at:

(1) Under the same load, the horizontal displacement of pile top in the test group with 6D loading height is larger than that in the test group with 2.1D loading height. The order of soil shear strength from weak to strong is as follows: saturated coarse sand, saturated fine sand, dry coarse sand, and dry fine sand. The difference in shear modulus among dry fine sand, dry coarse sand, and saturated fine sand is small, while the shear modulus of saturated coarse sand decreases sharply. The larger the particle size under saturated condition, the larger the pore water flow channel, which leads to a large attenuation of soil shear modulus.

(2) Under the same loading height and horizontal displacement of pile top, the maximum horizontal displacement of pile body below the surface, the maximum bending moment of pile body and the maximum soil resistance of pile body are in line with the relationship between soil stiffness. The relative stiffness of pile and soil has greater influence on the horizontal displacement of pile, in comparison with the influence of loading height. The loading height still has a certain influence on the bending moment and soil resistance distribution of the pile. The

bending moment and soil resistance distribution of the 6D loading height test group is larger than that of the 2.1D loading height test group, but the soil resistance distribution near the surface under 2.1D loading height above the zero point of soil resistance will be slightly larger than that of the 6D loading height test group under the same relative stiffness of pile and soil.

(3) With the increase of horizontal displacement of pile top, the zero depth of horizontal displacement of pile body is close to 0.25 m depth of pile body; At the same time, the increase of horizontal load causes the maximum bending moment of pile to move down from the buried depth of 0.2 m-0.25 m to 0.25 m-0.3 m.

(4) In the laboratory model test, due to the limitation of pile length and the lack of soil stress field, different from the prototype pile, the soil resistance at the end of the pile is small while the soil resistance at the end of the test pile is large. Moreover,with the increase of load, pile end soil resistance is on the rise.

Data Availability

The data presented in this study are available upon request from the corresponding author.

Conflicts of Interest

The authors declare that they have no conflicts of interest regarding the publication of this paper.

Acknowledgments

The authors would gratefully like to acknowledge the support provided by the National Natural Science Foundation of China (No. 51978177, 41902288), by the MOE Key Lab of Disaster Forecast and Control in Engineering, Jinan University (No. 20200904009). The editorial help from Professor Galen Leonhardy of Black Hawk College is also greatly appreciated.

References

[1] C. Lin and R. Wu, "Evaluation of vertical effective stress and pile lateral capacities considering scour-hole dimensions," *Canadian Geotechnical Journal*, vol. 56, no. 1, pp. 135–143, 2019.

[2] Li Yang, S. Wu, and S. Zhang, "Linear equation solution and application analysis of pile response under horizontal loading," *Journal of Geotechnical Engineering*, vol. 42, no. S1, pp. 70–74, 2020.

[3] B. Yuan, M. Sun, L. Xiong, Q. Luo, S. P. Pradhan, and H. Li, "Investigation of 3D deformation of transparent soil around a laterally loaded pile based on a hydraulic gradient model test," *Journal of Building Engineering*, vol. 28, no. 3, Article ID 101024, 2020.

[4] M. Yang, F. Chaobo, and M. Zhao, H. Luo, Calculation method of horizontal loaded pile strain wedge considering slope effect," *Geotechnical mechanics*, vol. 39, no. 4, pp. 1271–1280, 2018.

[5] R. Nandhagopal and K. Muthukkumaran, "Effect of rock-socketing on laterally loaded piles installed in the proximity of sloping ground," *International Journal of Geomechanics*, vol. 21, no. 2, Article ID 04020252, 2021.

[6] J. Jiang, C. Fu, and S. Wang, "Analytical method for soil resistance around horizontally loaded piles considering actual distribution," *Engineering Mechanics*, vol. 38, no. 11, pp. 199–211, 2021.

[7] B. Yuan, Z. Li, Y. Chen et al., "Mechanical and microstructural properties of recycling granite residual soil reinforced with glass fiber and liquid-modified polyvinyl alcohol polymer," *Chemosphere*, vol. 286, Article ID 131652, 2022.

[8] B. Yuan, Z. Li, Z. Su, Q. Luo, M. Chen, and Z. Zhao, "Sensitivity of multistage fill slope based on finite element model," *Advances in Civil Engineering*, vol. 2021, pp. 1–13, 2021.

[9] B. D. Ding, Z. Y. Han, G. C. Zhang, X. Beng, and Y. Yang, "Flexural toppling mechanism and stability analysis of an anti-dip rock slope," *Rock Mechanics and Rock Engineering*, vol. 54, no. 8, pp. 3721–3735, 2021.

[10] B. Zhu, G. Xiong, J. Liu, and X. Sun, "Large diameter single pile horizontal loading centrifugal model test in sandy soil," *Geotechnical Engineering Journal*, vol. 35, no. 10, pp. 1807–1815, 2013.

[11] L. Zhang, B. Zhu, and Y. Sun, "Research on the determination method of critical buried depth of super large diameter single pile in sandy seabed under horizontal cyclic loading," *Industrial buildings*, vol. 48, no. 6, pp. 91–95, 2018.

[12] L. Han, L. Wang, X. Ding, H. Wen, X. Yuan, and W. Zhang, "Similarity quantification of soil parametric data and sites using confidence ellipses," *Geoscience Frontiers*, vol. 13, no. 1, Article ID 101280, 2022.

[13] B. Yuan, L. Xiong, L. Zhai et al., "Transparent synthetic soil and its application in modeling of soil-structure interaction using optical system," *Frontiers of Earth Science*, vol. 7276 pages, 2019.

[14] D. H. Chen, H. E. Chen, W. Zhang, J. Lou, and B. Shan, "An analytical solution of equivalent elastic modulus considering confining stress and its variables sensitivity analysis for fractured rock masses," *Journal of Rock Mechanics and Geotechnical Engineering*, 2021.

[15] U. Erdal and L. Mustafa, "Experimental investigation of the behaviour of the laterally loaded short piles," *Teknik Dergi*, vol. 24, no. 1, pp. 6257–6278, 2013.

[16] M. R. Mahmood, N. M. Salim, and M. H. Abood, "The behavior of laterally loaded single pile model in unsaturated cohesionless soil," *IOP Conference Series: Materials Science and Engineering*, vol. 454, no. 1, Article ID 012175, 2018.

[17] Li Sen, J. Yu, and M. Huang, "Centrifugal test of horizontal cyclic loading of single pile with different stiffness in saturated clay," *Geotechnical engineering report*, vol. 43, no. 5, pp. 948–954, 2021.

[18] B. Yuan, Z. Li, W. Chen et al., "Influence of groundwater depth on pile–soil mechanical properties and fractal characteristics under cyclic loading," *Fractal and Fractional*, vol. 6, no. 4, 198 pages, 2022.

[19] B. Yuan, C. Rui, G. Deng, T. Peng, Q. Luo, and X. Yang, "Accuracy of interpretation methods for deriving p–y curves from model pile tests in layered soils," *Journal of Testing and Evaluation*, vol. 45, no. 4, pp. 20150484–20151246, 2017.

[20] L. Wang, F. Guo, H. Yang, Y. Wang, and S. Tang, "Comparison of fly ash, PVA fiber, MgO and shrinkage-reducing admixture on the frost resistance of face slab concrete via pore structural and fractal analysis," *Fractals*, vol. 29, no. 2, Article ID 2140002, 2021.

[21] Y. Wu, J. Cui, J. Huang, W. Zhang, N. Yoshimoto, and L. Wen, "Correlation of critical state strength properties with particle shape and surface fractal dimension of clinker ash," *International Journal of Geomechanics*, vol. 21, no. 6, Article ID 04021071, 2021.

[22] L. Kong, F. Xiao, J. Fan, and Y. Chen, "Horizontal eccentric pile group p-multiplier calculation," *Geotechnical mechanics*, vol. 40, no. 12, pp. 4659–4667, 2019.

[23] B. Yuan, K. Xu, Y. Wang, R. Chen, and Q. Luo, "Investigation of deflection of a laterally loaded pile and soil deformation using the PIV technique," *International Journal of Geomechanics*, vol. 17, no. 6, Article ID 04016138, 2017.

[24] B. Yuan, Z. Li, Z. Zhao, H. Ni, Z. Su, and Z. Li, "Experimental study of displacement field of layered soils surrounding laterally loaded pile based on transparent soil," *Journal of Soils and Sediments*, vol. 21, no. 9, pp. 3072–3083, 2021.

[25] B. Yuan, M. Sun, Y. Wang, L. Zhai, Q. Luo, and X. Zhang, "Full 3d displacement measuring system for 3d displacement field of soil around a laterally loaded pile in transparent soil," *International Journal of Geomechanics*, vol. 19, no. 5, Article ID 04019028, 2019.

[26] M. Z. Gao, J. Xie, Y. N. Gao et al., "Mechanical behavior of coal under different mining rates: a case study from laboratory experiments to field testing," *International Journal of Mining Science and Technology*, vol. 31, no. 5, pp. 825–841, 2021.

[27] G. Mingzhong, H. Haichun, X. Shouning et al., "Discing behavior and mechanism of cores extracted from Songke-2 well at depths below 4,500 m," *International Journal of Rock Mechanics and Mining Sciences*, vol. 149, Article ID 104976, 2022.

[28] C. Cao, W. Zhang, J. P. Chen, B. Shan, S. Song, and J. Zhan, "Quantitative estimation of debris flow source materials by integrating multi-source data: a case study," *Engineering Geology*, vol. 291, Article ID 106222, 2021.

[29] H. Lin, G. Lei, L. Xu, and G. Lei, "Similar analysis on deformation characteristics of 1g model test of horizontal loading pile," *Journal of Central South University*, vol. 43, no. 9, pp. 3639–3645, 2012.

[30] L. Wang, X. Song, H. Yang, S. Tang, B. Wu, and W. Mao, "Pore structural and fractal analysis of the effects of MgO reactivity and dosage on permeability and F–T resistance of concrete," *Fractal and Fractional*, vol. 6, no. 2, 113 pages, 2022.

[31] B. Bai, Q. Nie, Y. Zhang, X. Wang, and W. Hu, "Cotransport of heavy metals and SiO2 particles at different temperatures by seepage," *Journal of Hydrology*, vol. 597, Article ID 125771, 2021.

[32] M. Y. Fattah, H. H. Karim, and M. K. Mohsen, "Dynamic behavior of pile group model in two – layer sandy soil subjected to lateral earthquake excitation," *Global Journal of Engineering Science and Research Management*, vol. 3, no. 8, pp. 57–80, 2016.

[33] L. Wang, G. Li, X. Li, H. Asad, S. Tang, and X. Lu, "Influence of reactivity and dosage of MgO expansive agent on shrinkage and crack resistance of face slab concrete," *Cement and Concrete Composites*, vol. 126, Article ID 104333, 2022.

[34] M. Y. Fattah, B. S. Zbar, and F. S. Mustafa, "Effect of soil saturation on load transfer in a pile excited by pure vertical vibration," *Proceedings of the Institution of Civil Engineers – Structures and Buildings*, vol. 174, no. 2, pp. 132–144, 2021.

[35] L. Tao, *Research on Horizontal Load Characteristics of Offshore Wind Turbine Jacket Foundation*, Zhejiang University, Zhejiang, China, 2015.

[36] Xu, *Research on Displacement Field of Layered Soil Around Horizontal Loaded Piles Based on PIV Technology*, Guangdong University of Technology, Guangzhou, China, 2018.

[37] L. Wang, X. Lu, L. Liu et al., "Influence of MgO on the hydration and shrinkage behavior of low heat Portland cement-based materials via pore structural andfractal analysis," *Fractal and Fractional*, vol. 6, no. 1, 40 pages, 2022.

[38] M. Y. Fattah, H. H. Karim, and M. K. M. Al-Recaby, "Vertical and horizontal displacement of model piles in dry soil with horizontal excitation," *Proceedings of the Institution of Civil Engineers – Structures and Buildings*, vol. 174, no. 4, pp. 239–258, 2021.

[39] J. Xiao, Z. Xu, Y. Murong et al., "Effect of chemical composition of fine aggregate on the frictional behavior of concrete–soil interface under sulfuric acid environment," *Fractal Fract*, vol. 6, no. 1, p. 22, 2021.

[40] Y. Guo, J. Xie, J. Zhao, and K. Zuo, "Utilization of unprocessed steel slag as fine aggregate in normal- and high-strength concrete," *Construction and Building Materials*, vol. 204, pp. 41–49, 2019.

[41] Y. C. Guo, Y. Y. Ye, G. Lin, J. F. Lv, Y. L. Bai, and J. J. Zeng, "Effective usage of high strength steel tubes: axial compressive behavior of hybrid FRP-concrete-steel solid columns," *Thin-Walled Structures*, vol. 154, Article ID 106796, 2020.

[42] B. B. Yang, S. Yuan, Y. Liang, and J. Liu, "Investigation of overburden failure characteristics due to combined mining: case study, Henan Province, China," *Environmental Earth Sciences*, vol. 80, no. 4, 2021.

[43] Q. Lin, "Analysis of horizontal deformation characteristics of rigid pile foundation of offshore wind turbines," *China Water Transport (Second Half)*, vol. 15, no. 8, pp. 323–326, 2015.

[44] X. Que, Z. Zhu, Z. Niu, and W. Lu, "Estimating the strength and deformation of columnar jointed rock mass based on physical model test," *Bulletin of Engineering Geology and the Environment*, vol. 80, no. 2, pp. 1557–1570, 2021.

[45] B. Bai, R. Zhou, G. Cai, W. Hu, and G. Yang, "Coupled thermo-hydro-mechanical mechanism in view of the soil particle rearrangement of granular thermodynamics," *Computers and Geotechnics*, vol. 137, no. 8, Article ID 104272, 2021.

[46] W. Feng, F. Liu, F. Yang, L. Li, and L. Jing, "Experimental study on dynamic split tensile properties of rubber concrete," *Construction and Building Materials*, vol. 165, pp. 675–687, 2018.

[47] L. Wang, R. Y. Luo, W. Zhang, M. Jin, and S. Tang, "Effects of fineness and content of phosphorus slag on cement hydration, permeability, pore structure and fractal dimension of concrete," *Fractals*, vol. 29, no. 02, Article ID 2140004, 2021.

[48] M. Y. Fattah, H. H. Karim, and M. M. Al-Recaby, "Investigation of the end bearing load in pile group model in dry soil under horizontal excitation," *Acta Geotechnica Slovenica*, vol. 18, pp. 79–106, 2021.

[49] Y. C. Guo, J. H. Zhang, G. M. Chen, and Z. H. Xie, "Compressive behaviour of concrete structures incorporating recycled concrete aggregates, rubber crumb and reinforced with steel fibre, subjected to elevated temperatures," *Journal of Cleaner Production*, vol. 72, pp. 193–203, 2014.

[50] B. B. Yang, S. Du, X. Zhao, D. Tang, and C. Yang, "Decision making of curriculum attainment degree for engineering geology based on fuzzy set theory," *Advances in Civil Engineering*, vol. 2021, pp. 1–6, 2021.

[51] B. B. Yang and Y. Liu, "Application of fractals to evaluate fractures of rock due to mining," *Fractal and Fractional*, vol. 6, no. 2, p. 96, 2022.